Chinese Chemical Letters 31 (2020) 787–791

Contents lists available at ScienceDirect

Chinese Chemical Letters

journal homepage: www.elsevier.com/locate/cclet

Communication

Near-infrared photothermal release of hydrogen sulfide from nanocomposite hydrogels for anti-inflammation applications

Yan Huang[a], Haifeng Li[a], Xiaoxiao He[a], Xiaohai Yang[a], Li Li[a], Songyang Liu[a], Zhen Zou[b], Kemin Wang[a,*], Jianbo Liu[a,*]

[a] State Key Laboratory of Chemo/Biosensing and Chemometrics, College of Chemistry and Chemical Engineering, Key Laboratory for Bio-Nanotechnology and Molecular Engineering of Hunan Province, Hunan University, Changsha 410082, China
[b] School of Chemistry and Food Engineering, Changsha University of Science and Technology, Changsha 410114, China

ARTICLE INFO

Article history:
Received 12 April 2019
Received in revised form 28 April 2019
Accepted 14 May 2019
Available online 18 May 2019

Keywords:
Hydrogen sulfide
Near-infrared light
Photothermal transduction
Nanocomposite hydrogels
Anti-inflammation

ABSTRACT

A novel near-infrared light photothemal-activated H_2S-donating nanocomposite hydrogel was developed, through combination of a thermo-labile H_2S donor and photothermal nanoparticles in agarose hydrogel. The polyethylenimine dithiocarbamate polymer, a thermo-labile compound, was synthesized as a novel H_2S donor. The combination of a thermo-labile hydrogen sulfide donor and photothermal nanoparticles enabled the generation of H_2S in agarose hydrogel upon irradiation with near-infrared light. The ability to modulate the photoirradiation for controlled generation and spatiotemporally release of H_2S are its specific advantages. This photothermal spatiotemporally controlled H_2S-releasing strategy was successfully applied to anti-inflammation treatment in a rat model, demonstrating its utility as a novel H_2S-based therapeutic approach.

Since its role as a neuron modulator was first revealed in 1996 [1], hydrogen sulfide (H_2S) has been recognized as a unique signalling molecule that exerts protective effects in mammals against a range of conditions and events, such as inflammation [2], Parkinson's disease [3], cancer [4] and dermal wounds [5]. Accordingly, the therapeutic potential of this gasotransmitter has stimulated wide interest in the development of H_2S-releasing agents (H_2S donors). In this regard, developing a strategy for controlled generation of H_2S with high spatiotemporal precision is hence critically important for optimization of the therapeutic effect of H_2S [6,7].

Several types of H_2S donors that release H_2S in response to stimuli such as external light [8], pH [9], reactive oxygen species [10] and enzymatic activity [11]. have been reported. Among these strategies, light-induced H_2S release has gained considerable attention because of its ability to provide spatiotemporal control over H_2S release. Furthermore, controlling the period and intensity of the light irradiation can modulate the extent of H_2S release and its duration [12,13]. Photothermal triggering, as one of the light stimuli system, has emerged as a particularly promising technique for controlled release applications because of its biological benignity and convenient operation [14]. Photothermal release typically involves the application of plasmonic nanoparticles (pNPs) [15]. However, to the best of our knowledge, there are no reports on the use of pNPs for photothermally triggering H_2S release in specific spatial and temporal patterns.

Dithiocarbamate (DTC) compounds are thermo-labile organosulfur compounds that are capable of H_2S generation upon thermal pyrolysis [16]. Accordingly, we reasoned that if DTC compounds were combined with pNPs, the pNPs would convert incident light into heat and trigger the thermal decomposition of the guest molecules. Thus, a new light-driven H_2S-releasing platform based on photothermal transduction could be established.

To demonstrate the feasibility of this concept, here we present the use of near-infrared (NIR) light-driven photothermally responsive nanocomposites for H_2S release. Our H_2S-releasing system consists of thermo-labile polyethylenimine dithiocarbamate (PEI-DTC) polymers as H_2S donors and pNPs as NIR photothermal antennae combined in agarose hydrogel. As illustrated in Fig. 1, the dithiocarbamate addition reaction between polyethylenimine (PEI) and carbon disulfide (CS_2) results in the formation of a PEI-DTC polymer, which decomposes into H_2S at elevated temperature. Au@Ag/Au core@shell alloyed pNPs were used as NIR light nanotransducers owing to their large absorption cross section and efficacious hyperthermia in the NIR window [17]. Under 780 nm NIR photoirradiation, Au@Ag/Au pNPs absorb

* Corresponding authors.
E-mail addresses: kmwang@hnu.edu.cn (K. Wang), liujianbo@hnu.edu.cn (J. Liu).

https://doi.org/10.1016/j.cclet.2019.05.025
1001-8417/

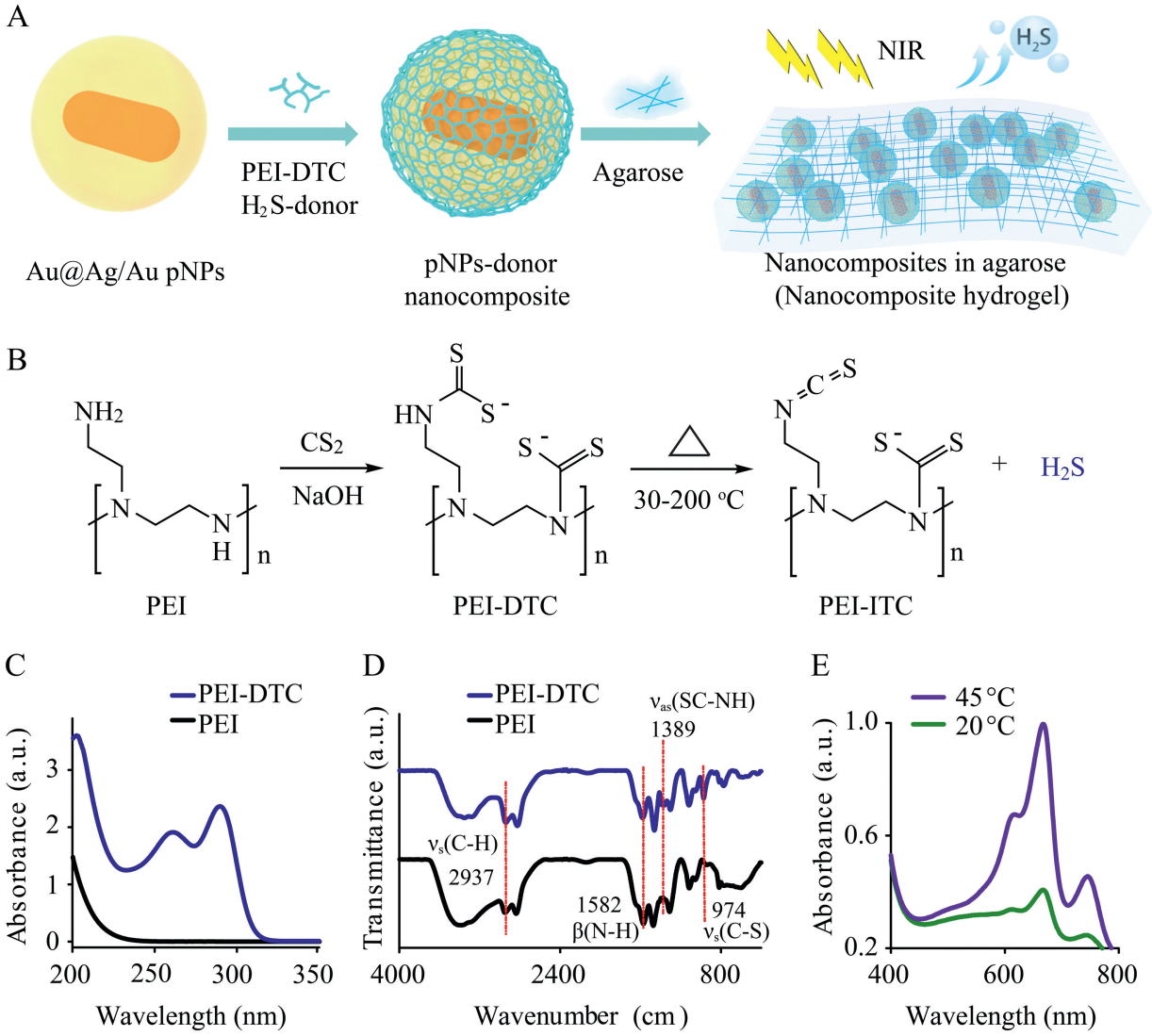

Fig. 1. Photothermally controlled generation of H_2S from nanocomposite agarose hydrogels. (A) PEI-DTC polymer H_2S donors are adsorbed on the surface of Au@Ag/Au pNPs and then loaded into agarose hydrogel. NIR photoirradiation triggers the release of H_2S through photothermal transduction. (B) Schematic of PEI-DTC preparation and its thermal decomposition. Decomposition of the monoalkyl dithiocarbamate fragment at 30-200 °C generates of H_2S. (C) UV–vis absorption spectra and (D) FTIR spectra of PEI-DTC and PEI polymers. (E) Methylene blue colorimetric analysis of H_2S generated from the thermal decomposition of PEI-DTC at 45 °C for 350 min (20 °C employed as a control temperature).

photoirradiation and converted it to thermal energy, initializing the thermal decomposition of the PEI-DTC polymer donor and thus generating H_2S (Fig. 1A). The loading of the photothermal donors in agarose hydrogel allows a spatiotemporally controlled approach for the photothermal generation of H_2S at concentrations in the micromolar range. The biological utility of our photothermal H_2S-donating system was demonstrated by treating the inflammation of rat toes. Our system uniquely combines the features of the strong photothermal reactivity of pNPs and a thermo-labile H_2S polymer donor. The ability to modulate the photoirradiation for controlled generation and spatiotemporally release of H_2S are its specific advantages.

Our fabrication of the thermo-labile H_2S-donor polymer PEI–DTC is based on dithiocarbamate condensation of CS_2 with the primary and secondary amine groups in the branched PEI polymer under basic conditions (Fig. 1B) [18]. The reaction of the PEI with excess CS_2 (CS_2/PEI = 1:8, w/w) at pH 7.0~9.0 yielded the PEI–DTC polymer as the major product (>90%). The photophysical properties of this polymer were investigated. Two new absorption peaks at 260 and 290 nm, which are characteristic absorptions of dithiocarbamate, are observed (Fig. 1C) [19]. The formation of PEI–DTC neutralized the positive charge of the polymer from 15.3 ± 1.2 mV to 4.9 ± 1.3 mV (Fig. S1 in Supporting information). The formation of PEI–DTC was further confirmed by FTIR and ^{13}C NMR. The FTIR spectrum of PEI–DTC presents new bands at 1389 cm^{-1} and 974 cm^{-1}, which are characteristic bending vibrations of the CS–NH bonds and C–S bonds in the dithiocarbamate, respectively (Fig. 1D). Compared with the ^{13}C NMR spectrum of PEI, a new chemical shift at 211 ppm appears in that of PEI–DTC, which is assigned to the dithiocarbamate (Fig. S2 in Supporting information). Thus, the above results confirm the formation of PEI–DTC, consistent with our previous results [20].

We next examined the thermal decomposition of the PEI-DTC H_2S donor using thermogravimetric analysis (TGA). PEI-DTC powder exhibits rapid weight loss in the temperature ranges 30~200 °C and 240~390 °C (Fig. S3 in Supporting information)). Monoalkyl dithiocarbamates were reported to exhibit high thermal labilities [21]. The weight loss in the temperature range (30~200 °C), which corresponds to decomposition of the primary-amine-derivatized monoalkyl dithiocarbamate fragment, is likely

to be responsible for the generation of H_2S (Fig. 1D). To verify this, the PEI-DTC was heated at 45 °C for 530 min (Fig. S4 in Supporting information)) and the pyrolytic products were collected for H_2S determination, which was performed using a standard methylene blue assay (Fig. S5 in Supporting information)) [22]. A remarkable increase in colorimetric adsorption at 667 nm was observed compared with that of the control (*i.e.*, the product mixture collected at 20 °C) (Fig. 1E), which clearly confirms that the elevated temperature facilitates the thermal decomposition of PEI-DTC and the generation of H_2S. In our system, the largest amount of H_2S released from the polymer donor was 33.2 μg from 1.0 mg PEI-DTC at 100 °C for 4 h (Fig. S6 in Supporting information)).

Having confirmed that the thermal decomposition of PEI-DTC provides H_2S, we sought to devise a photothermally responsive system in which a H_2S donor is combined with pNPs and loaded into agarose hydrogel. The Au@Ag/Au pNPs were prepared according to our previous protocol [17]. Transmission electron microscopy (TEM) and energy dispersive X-ray spectrometry (EDS) confirmed the successful preparation of the pNPs, which were observed to have an average diameter of 40.2 ± 5.7 nm and a core-shell structure morphology with a Au nanorod core and a Ag/Au alloy shell (Fig. 2A and inset of Fig. 2B). The nanoparticles exhibit strong UV-vis-NIR plasmonic adsorption in the wavelength range 400-1000 nm, indicative of pNPs that exhibit a strong photothermal response (Fig. 2B). The PEI-DTC was adsorbed onto the pNPs through electrostatic adsorption or coordination interaction, leading to the formation of donor-pNPs nanocomposites. Saturated adsorption of the PEI-DTC polymer onto the pNPs reverses their zeta potential, which changes from −18.4 ± 2.0 mV to 16.0 ± 2.4 mV (Fig. S7 in Supporting information). Hydrodynamic size of Au@Ag/Au pNPs was determined by dynamic light scattering (DLS), which revealed that their size increased from 43.6 ± 3.3 nm to 52.5 ± 2.5 nm after coating of PEI-DTC polymer (Fig. S8 in Supporting information). A maximum loading capacity of 1.12 mg PEI-DTC per mg of pNPs at room temperature was determined through a Langmuir equilibrium isotherm experiment (Fig. S9 in Supporting information).

The encapsulation of the nanocomposites into biologically inert agarose hydrogel would allow spatiotemporally localized gas release, which would be highly convenient for biomedical applications [23,24]. With this in mind, we loaded the donor-pNPs nanocomposites into agarose hydrogel. Fig. 2C shows five nanocomposite hydrogels loaded with different amounts of the pNPs-polymer nanocomposite (0~2.70 mg/g). The loading of nanocomposites causes a colour change in the hydrogel from white to brown. The morphology of the nanocomposite hydrogel was investigated by SEM (Fig. 2D). The nanocomposite hydrogel is assembled from thin wrinkled layers with a spatial network structure, and the layers are decorated with pNPs. As illustrated by the magnified image in Fig. 2E, the pNPs distributed on the hydrogel layers are estimated to be 45.0 ± 6.2 nm in diameter and are therefore likely to be the pNPs.

The photothermal properties of the nanocomposite hydrogels were investigated through photothermal imaging experiments. As shown in Fig. 3A, the hydrogel temperature gradually increases with illumination time, with an increase in nanocomposite loading facilitating temperature elevation. The quantitative photothermal responsive curves shown in Fig. 3B demonstrate that a nanocomposite loading of 2.70 mg/g results in a temperature increase from 20.2 °C to 45.5 °C upon NIR illumination for 10 min.

The photothermal effect facilitates the thermal decomposition of the polymer donor and the generation of H_2S from the nanocomposite hydrogel. After NIR illumination, strong fluorescence is observed from a nanocomposite hydrogel stained with the H_2S fluorescence probe 7-azido-4-methylcoumarin (AzMC) (Fig. S10 in Supporting information), which confirms the photothermal generation of H_2S in the hydrogels. Colorimetric quantitative analysis showed that the amount of H_2S released from the hydrogel gradually increases with illumination time, and higher nanocomposite loading facilitates the photogeneration of H_2S (Fig. 3C and Fig. S11 in Supporting information), which is

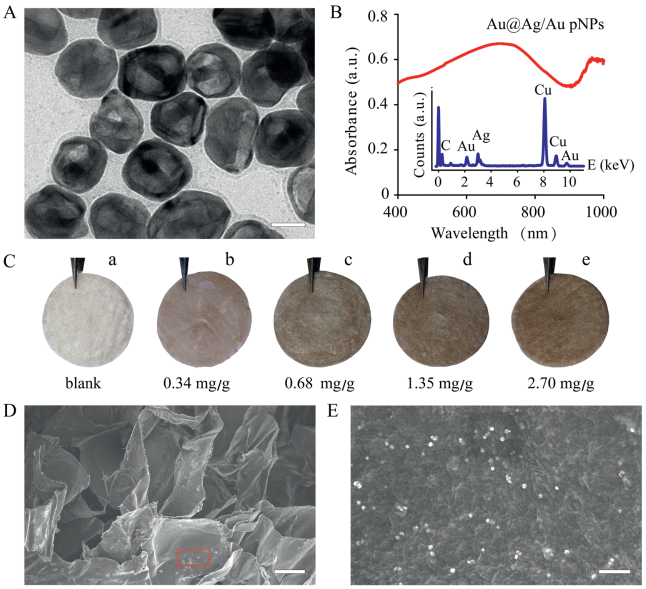

Fig. 2. (A) TEM image, (B) UV–vis absorption spectrum, and EDS analysis of Au@Ag/Au pNPs (inset). (C) Hydrogels loaded with different amounts of nanocomposite. (D) SEM image of a nanocomposite hydrogel. (E) Magnification of the red rectangle in (D). Scale bar: 20 nm (A), 50 μm (D) and 400 nm (E).

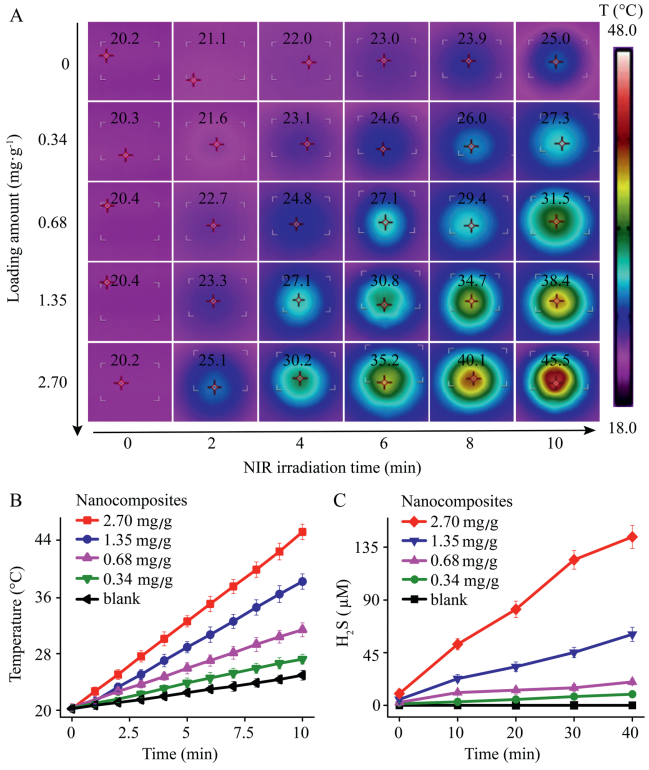

Fig. 3. (A) Thermal images of nanocomposite hydrogels loaded with different amounts of nanocomposite (0~2.70 mg/g) upon NIR (3.18 W/cm^2) illumination for different durations. (B) Quantitative temperature change plot of the data presented in (A). (C) Time-dependent H_2S generation from hydrogels loaded with different amounts of nanocomposite (0~2.70 mg/g).

consistent with the fluorescent hydrogel imaging results (Fig. S12 in Supporting information). The agarose hydrogel loaded with nanocomposite at 2.70 mg/g exhibits an increase in H_2S concentration to 144.0 μmol/L under 780 nm laser illumination for 40 min (Fig. 3C).

In our system, a H_2S-releasing polymer donor, photothermal pNPs, and light illumination are the three essential requirements for the photothermal generation of H_2S. Removal of one of these components stops the generation of H_2S, as confirmed by control experiments (Figs. S13 and S14 in Supporting information). NIR photoirradiation of the hydrogel containing both NPs and the H_2S donor leads to the generation of H_2S at 82.0 μmol/L, which is far higher than that by the hydrogel in the absence of pNPs (36.8 μmol/L) (Fig. S13). The results also provide compelling evidence that the photothermal pNPs are largely responsible for the generation of H_2S.

The prime advantage of this photothermal H_2S-releasing system is the convenient modulation of the excitation illumination for H_2S generation. When the nanocomposite hydrogel is irradiated at different laser powers, H_2S generation is modulated accordingly. For example, when nanocomposite irradiation at 3.18 W/cm^2 is stopped after 15 min, the H_2S production rate decelerates from 2.41 μmol L^{-1} min^{-1} to 0.12 μmol L^{-1} min^{-1} over 50 min. However, the production rate is restored to 0.93 μmol L^{-1} min^{-1} when laser excitation is restarted (Fig. S15 in Supporting information). High-power laser photon illumination facilitates the rapid generation of H_2S. For example, when the excitation power is increased stepwise from 0.06 W/cm^2 to 3.60 W/cm^2, the H_2S generation rate increases from 0.8 μmol L^{-1} min^{-1} to 2.3 μmol L^{-1} min^{-1} (Fig. S15). Thus, our system provides a facile and versatile platform for tuneable and spatiotemporally controlled H_2S release using NIR laser irradiation.

Because H_2S can induce neutrophil apoptosis and contribute to anti-inflammation [25], we further evaluated the ability of our photothermal H_2S-releasing platform to alleviate inflammation under NIR irradiation. The anti-inflammation experiment was conducted based on rat toe volume measurements (Fig. 4A) [26]. Typically, egg albumin was injected into a rat toe to induce local inflammation. Egg albumin injection causes edema in the toe of the rat and an emergence of swelling, indicative of the occurrence of inflammation (Fig. 4B). Then, a nanocomposite hydrogel (loading content 2.70 mg/g) was applied to the swollen area of the toe and subjected to NIR irradiation. A polymer donor-free agarose hydrogel was used as a control (Fig. S16 in Supporting information). Nanocomposite hydrogel has good biosafety, and no obvious cytotoxicity was observed for treatment with cells, which was proved by cell viability tests to quantitatively test the cytotoxicity of the nanocomposite hydrogel (Fig. S17 in Supporting information).

Photothermal generation of H_2S was confirmed by an AzMC fluorescent probe, which presented a strong blue fluorescence in the nanocomposite hydrogel but no discernible fluorescence in the H_2S-donor-free control hydrogel (Fig. 4C). After H_2S-releasing treatment, the volume of the swollen toe gradually decreased (Fig. 4B), as evaluated by measuring the volume change of the rat

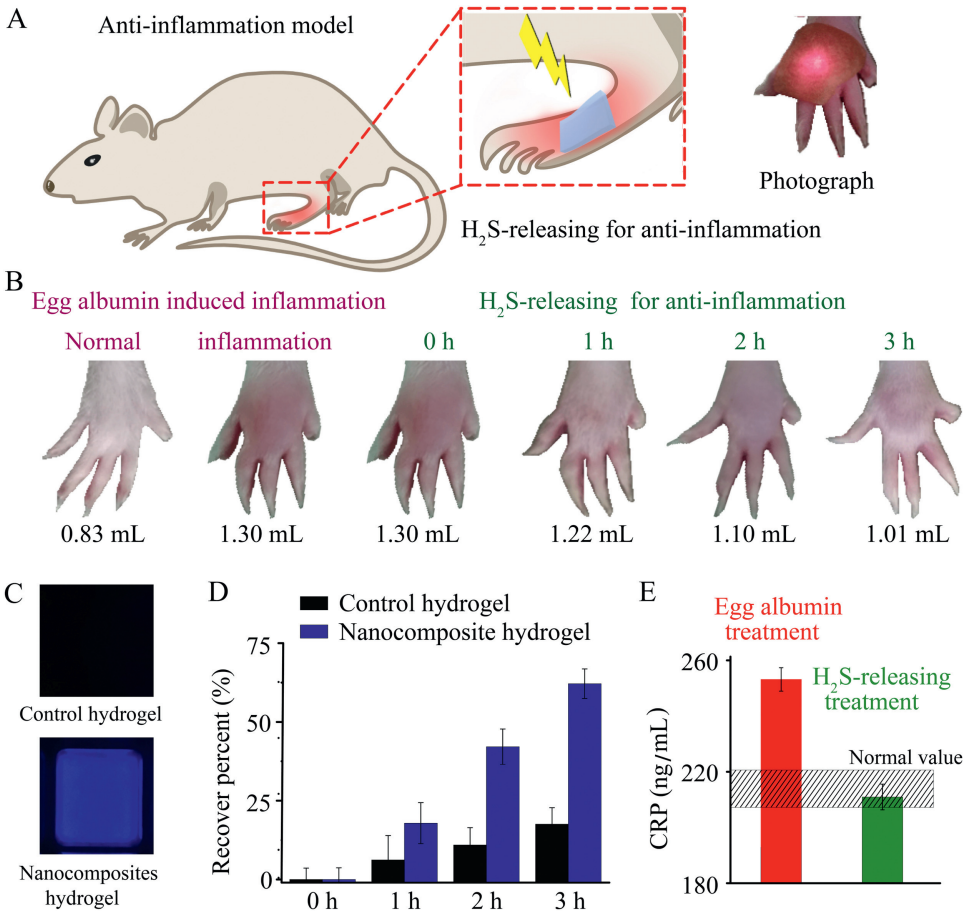

Fig. 4. *In vivo* anti-inflammation evaluation of nanocomposite hydrogel treatment. (A) Schematic of the rat model employed. (B) Rat toes in different conditions (normal, egg albumin treatment, and following H_2S-releasing treatment for different time intervals). (C) Fluorescence detection of the photothermal generation of H_2S in a hydrogel using an AzMC probe. (D) Recovery percent of the rat toe volumes under H_2S releasing treatment. (E) Quantitative expression of CRP in rat blood before and after treatment with nanocomposite hydrogels.

toe (Fig. S18 in Supporting information). As shown in Fig. 4B, photothermal release of H_2S alleviates the inflammation, leading to a gradual decrease in the toe volume. After H_2S-releasing treatment for 3.0 h, the toe volume decreased from 1.30 mL to 1.01 mL, constituting a recovery percentage value of 62.1%, which is far higher than the value of 17.6% observed for the control hydrogel (Fig. 4D).

In order to confirm that the toe volume change was associated with the alleviation of inflammation, C-reactive protein (CRP), a substance produced by the liver in response to inflammation, was determined through the enzyme-linked immunosorbent assay method. As illustrated in Fig. 4E, the CRP content of the rat blood increases rapidly to 253.2 ± 4.2 ng/mL upon egg albumin treatment. As expected, upon H_2S-releasing treatment, the CRP content decreases to 211.0 ± 4.6 ng/mL, which is located in the normal concentration range. Therefore, the results clearly demonstrate that the photothermal H_2S-releasing system has effective anti-inflammatory functionality.

In summary, a novel NIR-activated H_2S-donating nanocomposite hydrogel was developed. This strategy represents the first example of H_2S release upon photothermal triggering using pNPs as NIR antennae. PEI-DTC donors were assembled on the pNPs, which were then loaded into agarose hydrogel. The release of H_2S could be modulated in terms of spatial and temporal control by changing the irradiation parameters. In addition, the system was demonstrated to be capable of alleviating inflammation in rat toes. This work provides a new approach to the construction of photothermally sensitive H_2S-release systems and demonstrates the potential utility of these complexes as innovative drugs for the treatment and prevention of serious medical conditions.

Acknowledgments

The authors gratefully acknowledge the financial support of the National Natural Science Foundation of China (Nos. 21735002, 21575037, 21778016, 21675046 and 21877030), Natural Science Foundation of Hunan Province (No. 2177JJ3026), Keypoint Research and Invention Program of Hunan Province (No. 2017DK2011).

Appendix A. Supplementary data

Supplementary material related to this article can be found, in the online version, at doi:https://doi.org/10.1016/j.cclet.2019.05.025.

References

[1] K. Abe, H. Kimura, J. Neurosci. 16 (1996) 1066–1071.
[2] M. Li, J. Li, T. Zhang, et al., Eur. J. Med. Chem. 138 (2017) 51–65.
[3] X. Cao, L. Cao, L. Ding, J. Bian, Mol. Neurobiol. 55 (2018) 3789–3799.
[4] Y. Liu, F. Yang, C. Yuan, et al., ACS Nano 11 (2017) 1509–1519.
[5] J. Wu, Y. Li, C. He, et al., ACS Appl. Mater. Interfaces 8 (2016) 27474–27481.
[6] S. Gao, G. Tang, D. Hua, et al., J. Mater. Chem. B 7 (5) (2019) 709–729.
[7] Z. Xiao, T. Bonnard, A. Shakouri-Motlagh, et al., Chem. -Eur. J. 23 (2017) 11294–11300.
[8] S.Y. Yi, Y.K. Moon, S. Kim, et al., Chem. Commun. 53 (2017) 11830–11833.
[9] J. Kang, Z. Li, C.L. Organ, et al., J. Am. Chem. Soc. 138 (2016) 6336–6339.
[10] Y. Zhao, M. Pluth, Free Radic. Biol. Med. 128 (2016) 14858–14862.
[11] C.R. Powell, J.C. Foster, B. Okyere, M.H. Theus, J.B. Matson, J. Am. Chem. Soc. 138 (2016) 13477–13480.
[12] V. Yarra, J. Das, A. Chaudhuri, et al., Chem. Commun. 54 (2018) 3106–3109.
[13] W. Chen, M. Chen, Q. Zang, et al., Chem. Commun. 51 (2015) 9193–9196.
[14] J. Chen, C. Ning, Z. Zhou, et al., Prog. Mater. Sci. 99 (2019) 1–26.
[15] P. Lester, Z. Wesley, H. Dennis, et al., ACS Nano 4 (2010) 6395–6403.
[16] A.K. Sharma, Thermochim. Acta 104 (1986) 339–372.
[17] X. Ye, S. Hui, X. He, et al., J. Mater. Chem. B 2 (2014) 3667–3673.
[18] W. Zierkiewicz, M. Michalczyk, D. Bienko, D. Michalska, T. Zeegers-Huyskens, Int. J. Quantum Chem. 117 (2017) e25369.
[19] Y. Zhang, A.M. Schnoes, A.R. Clapp, ACS Appl. Mater. Interfaces 2 (2010) 3384–3395.
[20] L. Li, J. Liu, X. Yang, et al., Nanotechnology 27 (2016) 105603.
[21] S. Kanchi, P. Singh, K. Bisetty, Arab. J. Chem. 7 (2014) 11–25.
[22] N.S. Lawrence, J. Davis, L. Jiang, et al., Electroanalysis 12 (2000) 1453–1460.
[23] Y. Zou, L. Zhang, L. Yang, et al., J. Controlled Release 273 (2018) 160–179.
[24] S. Li, S. Dong, W. Xu, et al., Adv. Sci. 5 (2018) 1700527.
[25] B. Gemici, J.L. Wallace, Methods Enzymol. 555 (2015) 169–193.
[26] H.Y. Chang, M.J. Sheu, C.H. Yang, et al., Evid. Based Compl. Alt. Med. 17 (2011) 9112–9119.